IOP Publishing Semiconductor Science and Technology
Semicond. Sci. Technol. 25 (2010) 015002 (8pp) doi:10.1088/0268-1242/25/1/015002

Determination of diode parameters of a silicon solar cell from variation of slopes of the *I–V* curve at open circuit and short circuit conditions with the intensity of illumination

Firoz Khan[1,3], S N Singh[1] and M Husain[2]

[1] Electronic Materials Division, National Physical Laboratory, New Delhi, India
[2] Department of Physics, Jamia Millia Islamia, New Delhi, India

E-mail: firozkphysics@gmail.com

Received 10 May 2009, in final form 7 November 2009
Published 1 December 2009
Online at stacks.iop.org/SST/25/015002

Abstract
An analytical method of determination of all the four diode parameters of the single exponential model of a silicon solar cell, namely shunt resistance R_{sh}, series resistance R_s, diode ideality factor n and reverse saturation current I_0 from the variation of slopes of the *I–V* curve of the cell near short circuit and open circuit conditions with intensity of illumination in a small range of intensity, is presented for the first time. In a suitable range of intensity the variation of $\mathrm{d}I/\mathrm{d}V$ at short circuit enables determination of R_{sh}, whereas the variation of $\mathrm{d}I/\mathrm{d}V$ at open circuit enables determination of R_s, n and I_0. The diode parameters of a silicon solar cell were determined with this method using *I–V* characteristics of the cell in 40–125 mW cm^{-2} intensity range of a simulated AM1.5 solar radiation. Theoretical *I–V* curves generated using so determined values of the diode parameters matched well with the experimental *I–V* curves of the cell obtained under various intensities of illumination in the above range.

Introduction

The steady state *I–V* characteristics of a p–n junction silicon solar cell are often described based on a single exponential model [1–4]:

$$I = -I_{ph} + I_0\left(\mathrm{e}^{\frac{q(V-IR_s)}{nkT}} - 1\right) + \frac{V - IR_s}{R_{sh}}. \qquad (1)$$

In equation (1) I_{ph} is the light-generated current, q is the electron charge, k is the Boltzmann constant, T is the temperature, R_{sh} is the shunt resistance, R_s is the series resistance, n is the diode ideality factor and I_0 is the reverse saturation current of the cell. R_{sh}, R_s, n and I_0 are diode parameters of the cells.

The performance of a solar cell is monitored through four performance parameters, i.e. open circuit voltage (V_{oc}), short circuit current (I_{sc}), curve factor (CF) and efficiency (η) of the cell but the diode parameters decide the values of the performance parameters at a given intensity P_{in} and temperature. Despite the diode parameters remaining constant, the values of performance parameters change as the intensity changes. In general, I_{sc} increases linearly, whereas V_{oc} increases logarithmically with P_{in} [5–7]. However, CF and η first increase with P_{in} and, then, decrease after a certain value of P_{in} [5–7].

Many analytical methods have been developed to determine one or more of the diode parameters [1, 8–13]. However, none of the above analytical methods is able to determine all the diode parameters of a cell. Therefore, one has to generally use three or four methods to determine all the diode parameters. But since each method has a different physical basis they are rarely compatible. Consequently the values of R_{sh}, R_s, n and I_0 obtained using them are not likely to be correct values of the diode parameters to describe the *I–V* characteristics of the cell accurately.

[3] Author to whom any correspondence should be addressed.

Some numerical or curve fitting techniques have been applied to extract all diode parameters from a single *I*–*V* curve obtained under illumination conditions [14–18]. Each of these methods [15–18] uses a single *I*–*V* curve and requires special computational knowledge to determine the values of all the diode parameters of a cell. These methods have a severe drawback in that using two close *I*–*V* curves (such as those obtained at two slightly different intensities of illumination), they give quite different values of the diode parameters and one is not sure about the correct values [18].

In this paper a new analytical method of measurement of all four diode parameters R_{sh}, R_s, n and I_0 of a single exponential model of a solar cell is presented. It is based on variation of the slope dI/dV of the *I*–*V* curve at short circuit and open circuit conditions with the change of incident light intensity and enables determination of not only R_{sh} and R_s but also n and I_0 of the cell accurately.

Theoretical details

Let us assume that the values of diode parameters R_{sh}, R_s, n and I_0 remain constant with I and V. Then differentiating equation (1), we get

$$\frac{\mathrm{d}I}{\mathrm{d}V} = \frac{\left[\frac{1}{R_{sh}} + \frac{q}{nkT}\left\{I_{ph} + I_0 - I\left(1 + \frac{R_s}{R_{sh}}\right) - \frac{V}{R_{sh}}\right\}\right]}{1 + R_s\left[\frac{1}{R_{sh}} + \frac{q}{nkT}\left\{I_{ph} + I_0 - I\left(1 + \frac{R_s}{R_{sh}}\right) - \frac{V}{R_{sh}}\right\}\right]}. \tag{2}$$

For the short circuit condition ($V = 0$, $I = I_{sc}$), equation (1) gives

$$I_{ph} + I_0 - I_{sc}\left(1 + \frac{R_s}{R_{sh}}\right) = I_0\,e^{\frac{qI_{sc}R_s}{nkT}} \tag{3}$$

and for the open circuit condition ($V = V_{oc}$, $I = 0$) it gives

$$I_{ph} + I_0 - \frac{V_{oc}}{R_{sh}} = I_0\,e^{\frac{qV_{oc}}{nkT}}. \tag{4}$$

Using equations (3) and (4) in equation (2) respectively and defining dI/dV at short circuit as m_{sc} and at open circuit as m_{oc} we obtain

$$m_{sc} = \frac{\left[\frac{1}{R_{sh}} + \frac{qI_0}{nkT}\,e^{\frac{qI_{sc}R_s}{nkT}}\right]}{\left[1 + R_s\left\{\frac{1}{R_{sh}} + \frac{qI_0}{nkT}\,e^{\frac{qI_{sc}R_s}{nkT}}\right\}\right]} \tag{5}$$

and

$$m_{oc} = \frac{\left[\frac{1}{R_{sh}} + \frac{qI_0}{nkT}\,e^{\frac{qV_{oc}}{nkT}}\right]}{\left[1 + R_s\left\{\frac{1}{R_{sh}} + \frac{qI_0}{nkT}\,e^{\frac{qV_{oc}}{nkT}}\right\}\right]}. \tag{6}$$

Equation (5) shows that m_{sc} is related to the diode parameters (R_{sh}, R_s, n and I_0) and I_{sc} of the cell. Similarly equation (6) shows that m_{oc} is related to the above diode parameters and V_{oc} of the cell. Since both I_{sc} and V_{oc} depend on the intensity of illumination P_{in} we can expect both m_{sc} and m_{oc} to change with P_{in}, whether or not the diode parameters change with P_{in}. Thus, equations (5) and (6) can be used to determine the values of the above diode parameters of a cell by measuring the slopes m_{sc} and m_{oc} at different intensities in a small range of intensity, wherein the diode parameters remain constant.

In a solar cell, the excess carrier concentration (or in other words the injection level n_o) increases linearly with P_{in}. Since most cells are made using silicon of more than 0.2 Ω cm resistivity, the Auger recombination in them is negligible. In such cells the variations of τ and D_n of minority carriers in p-base region of an n^+-p-p^+ solar cell and hence of n and I_0 with P_{in} is expected to be negligible over one or two orders of magnitude of P_{in} [19–24].

Because of the negligible contribution of the base region, the effect of P_{in} on R_s of such cells is also insignificant. Therefore, it is fair to consider diode parameters as constants in a small P_{in} range of less than one order of magnitude for cell operating under low-level conditions.

For some suitable P_{in} range equations (5) and (6) may further be simplified if the following conditions are satisfied simultaneously:

$$\frac{qI_0}{nkT}\,e^{\frac{qI_{sc}R_s}{nkT}} \ll \frac{1}{R_{sh}} \tag{7}$$

and

$$\frac{qI_0}{nkT}\,e^{\frac{qV_{oc}}{nkT}} \gg \frac{1}{R_{sh}}. \tag{8}$$

The left-hand side of inequality (7) stands for the diode conductance at short circuit condition, whereas, the left-hand side of inequality (8) stands for the diode conductance at open circuit condition. $1/R_{sh}$ represents the shunt conductance in both the inequalities. Thus, each of the above inequalities compares the diode conductance with the shunt conductance. In inequality (7) the diode conductance is much less than the shunt conductance, whereas in inequality (8) the diode conductance is much greater than the shunt conductance.

If we delineate the suitable P_{in} range as $P_{in1} < P_{in} < P_{in2}$, then, inequality (9) will define the higher intensity limit P_{in2} and inequality (10) will define the lower intensity limit P_{in1} of this suitable P_{in} range. We will determine P_{in1} and P_{in2} values a little later.

Conditions (7) and (8) being valid equations (5) and (6) get simplified to give, respectively,

$$m_{sc}^{-1} = (R_{sh} + R_s) \tag{9}$$

and

$$m_{oc}^{-1} = \left[R_s + \frac{nkT}{qI_0}\cdot e^{-\left(\frac{qV_{oc}}{nkT}\right)}\right]. \tag{10}$$

For most cases of practical interests [6] one finds that

$$R_s/R_{sh} \ll 1 \tag{11}$$

and

$$I_0\,e^{\frac{qI_{sc}R_s}{nkT}} \ll \left(I_{sc} - \frac{V_{oc}}{R_{sh}}\right). \tag{12}$$

Using inequalities (11) and (12) equation (3) gives $I_{sc} \approx I_{ph}$ and equations (3) and (4) yield

$$I_0\,e^{\frac{qV_{oc}}{nkT}} = \left(I_{sc} - \frac{V_{oc}}{R_{sh}}\right). \tag{13}$$

Substituting equation (13) into equation (10) we get

$$m_{oc}^{-1} = \left[R_s + \frac{nkT}{q}\cdot\frac{1}{\left(I_{sc} - \frac{V_{oc}}{R_{sh}}\right)}\right]. \tag{14}$$

Inequality (11) simplifies equation (9) to

$$R_{sh} = m_{sc}^{-1}. \tag{15}$$

Taking logarithm of both sides of equation (13) we also obtain the relation

$$V_{oc} = \frac{nkT}{q} \cdot \ln\left(I_{sc} - \frac{V_{oc}}{R_{sh}}\right) - \frac{nkT}{q} \cdot \ln(I_0). \tag{16}$$

Combination of equations (10) and (14)–(16) can be used to determine representative values of R_{sh}, R_s, n and I_0 of a cell from measurements of I_{sc}, V_{oc}, m_{sc} and m_{oc} at different intensities in a suitable P_{in} range in which inequalities (7), (8), (11) and (12) are well satisfied.

Determination of suitable intensity range

Let us denote V_{oc}, I_{sc} values which correspond to low intensity limit P_{in1} as V_{oc1}, I_{sc1} respectively and those which correspond to high intensity limit P_{in2} as V_{oc2}, I_{sc2} respectively. Then using inequalities (7) and (8) we can write

$$\left[\left(\frac{qI_0}{nkT}\,\mathrm{e}^{\frac{qI_{sc2}R_s}{nkT}}\right)\Big/\left(\frac{1}{R_{sh}}\right)\right] = \varepsilon_2 \tag{17}$$

and

$$\left[\left(\frac{1}{R_{sh}}\right)\Big/\left(\frac{qI_0}{nkT}\,\mathrm{e}^{\frac{qV_{oc1}}{nkT}}\right)\right] = \varepsilon_1 \tag{18}$$

which imply that $\varepsilon_1 \ll 1$ and $\varepsilon_2 \ll 1$.

In equation (18) ε_1 represents the ratio of shunt conductance to the diode conductance at open circuit whereas ε_2 represents the ratio of diode conductance at short circuit to the shunt conductance of the cell in equation (17). The value of ε_1 indicates the fraction of the error that has been allowed in obtaining equation (9) from equation (5). Similarly, the value of ε_2 indicates the fraction of the error that has been allowed in obtaining equation (10) from equation (6). Smaller the values of ε_1 and ε_2 better the validity of the method.

With assumptions (11) and (13), equation (3) yields $I_{ph} \approx I_{sc}$ which indicates that the validity of the method is restricted to the range where I_{sc} increases linearly with P_{in}. The lower intensity limit P_{in1} and the upper intensity limit P_{in2} of suitable intensity range may also be defined in terms of I_{sc1} and I_{sc2} respectively.

From equation (17) one can obtain I_{sc2} as

$$I_{sc2} = \frac{nkT}{qR_s} \cdot \ln\left[\frac{1}{R_{sh}} \cdot \frac{nkT}{qI_0} \cdot \varepsilon_2\right]. \tag{19}$$

Similarly combining equations (18) and (13) one can obtain I_{sc1} as

$$I_{sc1} = \frac{nkT}{qR_{sh}}.\left[\frac{1}{\varepsilon_1} + \ln\left(\frac{nkT}{qI_0\varepsilon_1 R_{sh}}\right)\right]. \tag{20}$$

Thus, the suitable intensity range defined by $P_{in1} < P_{in} < P_{in2}$ may also be represented in terms of the valid I_{sc} range as $I_{sc1} < I_{sc} < I_{sc2}$.

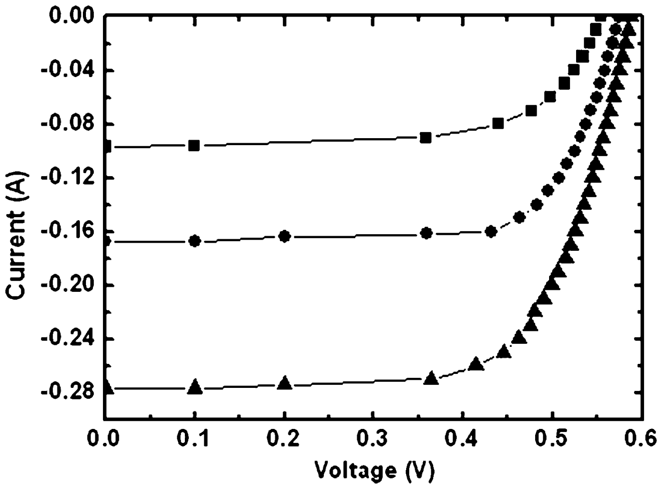

Figure 1. Illuminated *I–V* characteristics of cell 1 at 25 °C under three different intensities of simulated AM1.5 solar radiations in the 40–125 mW cm^{-2} range.

Experimental details

The measurements for the present work were made on monocrystalline silicon (c-Si) solar cells of an ∼8 cm^2 area which were fabricated using 300 μm thick ⟨100⟩ oriented p-Cz silicon wafer of 1 Ω cm base resistivity and the p–n junction was made by P-diffusion using the $POCl_3$ liquid source. Front and back contacts were realized by screen printing Ag paste on front and Ag/Al paste on backsides of the cells. A single layer silicon nitride antireflection coating was given by a PECVD process using SiH_4, NH_3 and N_2 gases. Illuminated *I–V* characteristics of the cells were measured at 25 °C under various intensities of illumination in 40–125 mW cm^{-2} range of simulated AM 1.5 solar radiations. A Keithley 2420 system sourcemeter was used for measurement of *I–V* characteristics and the intensity was measured using a reference silicon solar cell obtained from PV Measurements, USA. In the following the results of measurements are reported for a silicon solar cell, cell 1 fabricated as described above.

Result and discussion

Three experimental *I–V* characteristics of cell 1 obtained at 25 °C under three different intensities of illumination are shown in figure 1. We note that the slope dI/dV of each curve near open circuit is distinctly different. A number of such *I–V* curves were obtained in 40–125 mW cm^{-2} intensity range and were used to determine, m_{sc}, m_{oc}, V_{oc} and I_{sc} values for each curve which were in turn used to determine the diode parameters of the cell. The value of m_{sc} was nearly invariant with intensity and thereby yielded a constant value of R_{sh} according to equation (15). However, the values of R_s, n and I_0 could be determined from two different approaches A and B.

In approach A first the values of m_{oc}^{-1} are plotted against $(I_{sc}-V_{oc}/R_{sh})^{-1}$ as shown in figure 2 and are fitted into a straight line represented by equation (14). The intercept of the straight line on the m_{oc}^{-1} axis gave R_s and the slope of the line

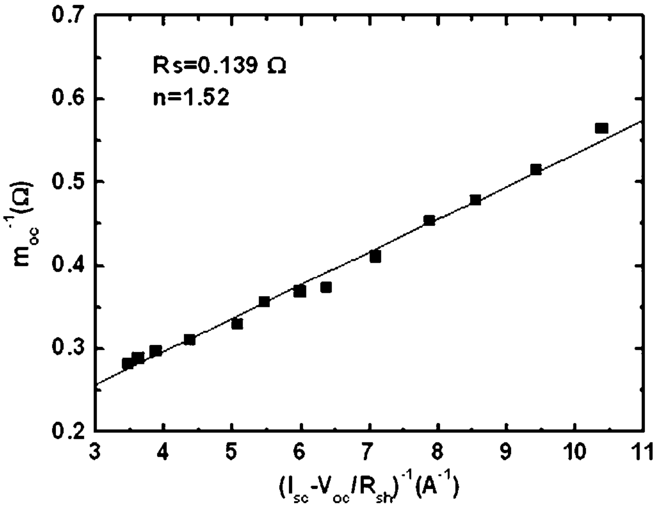

Figure 2. Plot of m_{oc}^{-1} versus $(I_{sc}-V_{oc}/R_{sh})^{-1}$ for cell 1 at $T = 25$ °C and $40 < P_{in} < 125$ mW cm^{-2}. The solid line gives a straight line fit to the data. The intercept of the line on the m_{oc}^{-1} axis gives R_s and the slope of the line from the $(I_{sc}-V_{oc}/R_{sh})^{-1}$ axis determines n.

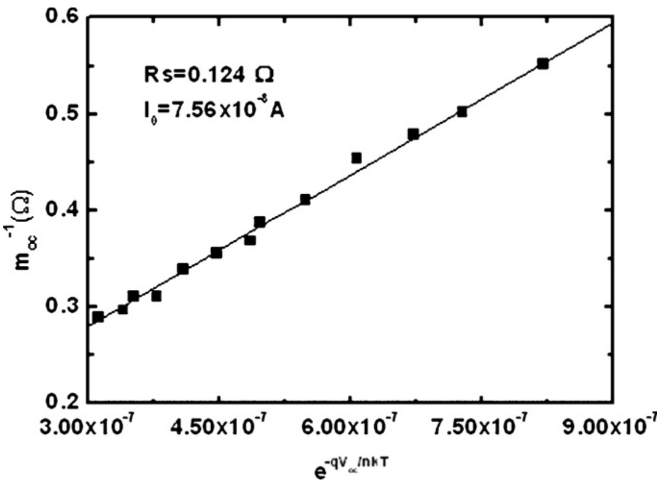

Figure 3. Plot of m_{oc}^{-1} versus $e^{-qV_{oc}/nkT}$ at $T = 25$ °C with $n = 1.52$; n was obtained from figure 2. The solid line gives a straight line fit to the data. The slope of straight line with the $e^{-qV_{oc}/nkT}$ axis determines I_0 value.

from the $(I_{sc}-V_{oc}/R_{sh})^{-1}$ axis yielded the value of nkT/q. The value of n thus obtained was used in equation (10) and, then, the plot of the m_{oc}^{-1} versus $e^{-qV_{oc}/nkT}$ data and their subsequent fit into a straight line as shown in figure 3 yielded the value of I_0 from its slope nkT/qI_0 with the $e^{-qV_{oc}/nkT}$ axis. The intercept of the m_{oc}^{-1} versus $e^{-qV_{oc}/nkT}$ line on the m_{oc}^{-1} axis of figure 3 also gave a value of R_s. This approach determines values of all four diode parameters using m_{sc} and m_{oc} values.

In approach B we first determined R_{sh} from m_{sc} data using equation (15) as discussed earlier. Then, we determined I_0 and n from a straight line obtained by plotting V_{oc} against $\ln(I_{sc}-V_{oc}/R_{sh})$ according to equation (16) as shown in figure 4. Subsequently, the value of n so obtained was used in equation (14) to determine R_s from the m_{oc}^{-1} versus $e^{-qV_{oc}/nkT}$ straight line graph similar to that of figure 3 (but not shown here) which also gave a value of I_0 from the slope. Thus, in

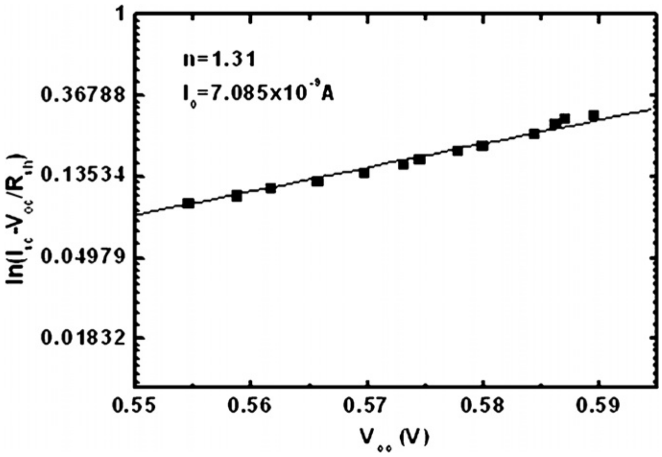

Figure 4. Plot of the ln $(I_{sc}-V_{oc}/R_{sh})$ versus V_{oc} axis for cell 1 at $T = 25$ °C and $40 < P_{in} < 125$ mW cm^{-2}. I_0 was determined from the intercept on the ordinate and n from the slope with the V_{oc} axis.

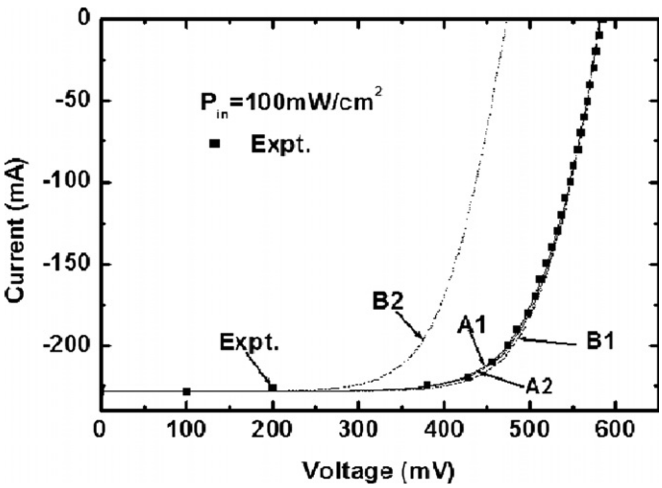

Figure 5. Plot of experimental and theoretical *I–V* curves for cell 1 at $T = 25$ °C. Theoretical curves A_1, A_2, B_1 and B_2 have been generated using the values of set A_1, A_2, B_1 and B_2 respectively given in table 2.

approach B, the m_{oc} data were not used for determination of n of the cell.

The values of R_{sh}, R_s, n and I_0 determined by the two approaches for cell 1 are given in table 1. It shows that approach A gave two different values of R_s, whereas approach B gave two different values of I_0. From table 1 four sets of values of the four diode parameters could be formed. These sets of values of R_{sh}, R_s, n and I_0 are listed in table 2.

Four theoretical *I–V* curves have been obtained using the four different sets of diode parameters of table 2 in equation (1) for $I_{sc} = 228.6$ mA that corresponded to 100 mW cm^{-2} intensity of the incident simulated AM1.5 solar radiation. These curves are plotted in figure 5 along with the experimental curve. Theoretical curves A_1, A_2, B_1 and B_2 correspond respectively to sets A_1, A_2, B_1 and B_2 of diode parameters listed in table 2. It can be noted that curves A_1, A_2 and B_1 are quite close to the experimental curves, whereas curve B_2 is far apart. This indicates that equations (10), (14)–(16) and the

Table 1. The values of diode parameters at $T = 25$ °C determined for cell 1 using approaches A & B.

	Value					
	Approach A			Approach B		
Diode parameters	Equation (15)	Equation (14) ($R_{sh} = 998$)	Equation (10) ($n = 1.52$)	Equation (15)	Equation (16) ($R_{sh} = 998$)	Equation (10) ($n = 1.31$)
R_{sh} (Ω)	998	–	–	998	–	–
R_{sh} (Ω)	–	0.139	0.124	–	–	0.153
n	–	1.52	–	–	1.31	–
I_0(A)	–	–	7.56×10^{-8}	–	7.09×10^{-9}	1.90×10^{-7}

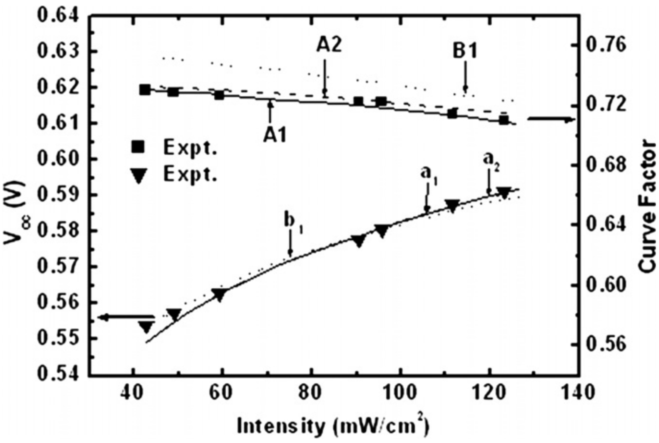

Figure 6. Variation of experimental and theoretical V_{oc} and CF at $T = 25$ °C for cell 1 with intensity in $40 < P_{in} < 125$ mW cm^{-2} range. Theoretical curves (a_1, A_1), (a_2, A_2) and (b_1, B_2) are based on sets A_1, A_2 and B_1 of table 2.

assumptions made in obtaining them have been fairly valid in cases of the A_1, A_2 and B_1 curves.

A closer look at the curves of figure 5 reveals that curve A_1 matches best with the experimental curve. This is evident also from the comparison of V_{oc} and CF values of the theoretical curves with the experimental curve of cell 1 at $I_{sc} = 228.6$ mA and $T = 25$ °C as given in table 3. From table 3 we observe that for curve B_2 the value of CF is comparable with the experimental CF value. However, the theoretical V_{oc} value for curve B_2 is very small in comparison with the experimental V_{oc} value. It shows that closeness of two *I–V* curves is revealed by V_{oc} and CF values together. Matching only CF values without V_{oc} may be misleading.

Similar observations were made by comparing theoretical and experimental *I–V* curves of cell 1 at other intensities. Figure 6 depicts variation of theoretical and experimental values of V_{oc} and CF of cell 1 at $T = 25$ °C with P_{in} in the 40–125 mW cm^{-2} range. There are three theoretical curves each for V_{oc} and CF. The CF versus P_{in} curves A_1, A_2 and B_1 have been obtained using the diode parameters of sets A_1, A_2 and B_1 respectively. Similarly, the V_{oc} versus P_{in} curves a_1, a_2 and b_1 correspond to the diode parameters of set A_1, A_2 and B_1 respectively. The V_{oc} versus P_{in} curves match reasonably well with the experimental values. Curves a_1 and a_2 are superposed. This is because for both these curves the values of the diode parameters R_{sh}, n and I_0 that together decide the value of V_{oc} are same. Theoretical curve A_1 matches closely with the experimental CF values. Curve A_2 lies slightly above A_1 indicating CF values that are not very significantly higher than the experimental values. On the other hand, curve B_1 shows much higher CF values than the experimental ones.

Table 2. Four sets of values of diode parameters of cell 1 at $T = 25$ °C formed using table 1.

Diode parameters	Set A_1	A_2	B_1	B_2
R_{sh} (Ω)	998	998	998	998
R_s (Ω)	0.139	0.124	0.153	0.153
n	1.52	1.52	1.31	1.31
I_0 (A) $\times 10^{-8}$	7.56	7.56	0.709	190

From above it becomes clear that approach A which uses the slopes of *I–V* curves at short circuit and open circuit conditions along with the I_{sc} values of the cell at different intensities provides most realistic values of diode parameters in the form of set A_1 using combination of equation (15) for R_{sh}, equation (14) for R_s and n and equation (10) for I_0. Table 4 shows that the assumptions (i.e. inequalities (7), (8), (11) and (12)) have been fairly valid for cell 1 in the 40–125 mW cm^{-2} intensity range. $P_{in} = 40$ mW cm^{-2} corresponded to $\varepsilon_1 = 0.0027$, whereas $P_{in} = 125$ mW cm^{-2} corresponded to $\varepsilon_2 = 0.0053$. Such small values of ε_1 and ε_2 in comparison with unity speak of excellent accuracy of the method in determining the diode parameters of cell 1.

With diode parameter values $R_{sh} = 998$ Ω, $R_s = 0.139$ Ω, $n = 1.52$ and $I_0 = 7.56 \times 10^{-8}$ A corresponding to curve A_1, the lower and upper intensity limits were calculated for $\varepsilon_1 = 0.01$ and $\varepsilon_2 = 0.01$ using equations (20) and (19) respectively. $\varepsilon_1 = 0.01$ gave $I_{sc1} = 4.37$ mA that corresponded to $P_{in1} = 1.91$ mW cm^{-2}. Likewise $\varepsilon_2 = 0.01$ gave $I_{sc2} = 467$ mA that corresponded to $P_{in2} = 204$ mW cm^{-2}. Thus, allowing $\varepsilon_1 = \varepsilon_2 = 0.01$ the valid intensity range for application of the present method is 1.91–204 mW cm^{-2}. This shows that the P_{in} range 40–125 mW cm^{-2} used for measurement in this work has been well within the valid P_{in} range. We shall henceforth refer approach A to determine the values of diode parameters as in set A_1 of table 2 as our method.

Comparison with other methods

Agarwal *et al* method [12] was not applicable for measurement of R_s for cell 1 in 40–125 mW cm^{-2} range as this method [12] required I_{sc} to be significantly lower than I_{ph} which was not

Table 3. Comparison of values of V_{oc} and CF for experimental and theoretical *I–V* curves of cell 1 at 25 °C obtained under a simulated AM1.5 solar radiation of 100 mW cm^{-2} intensity, using sets of diode parameters given in table 2.

P_{in}		Value for curves				
(mW cm^{-2})	Parameter	Experimental	A_1	A_2	B_1	B_2
100	V_{oc} (mV)	584.4	583.2	583.1	584	471.5
	CF	0.718	0.717	0.721	0.731	0.691

Table 4. The validity of assumptions for cell 1 at $T = 25$ °C and $40 < P_{in} < 125$ mW cm^{-2} intensity range.

	$R_S \ll R_{sh}$		$\frac{qI_0}{nkT}\,e^{\frac{qI_{sc}R_s}{nkT}} \ll \frac{1}{R_{sh}}$		$\frac{qI_0}{nkT}\,e^{\frac{qV_{oc}}{nkT}} \gg \frac{1}{R_{sh}}$		$I_0\,e^{\frac{qI_{sc}R_s}{nkT}} \ll \left(I_{sc} - \frac{V_{oc}}{R_{sh}}\right)$	
Curve	R_s (Ω)	R_{sh} (Ω)	$\frac{qI_0}{nkT}\,e^{\frac{qI_{sc}R_s}{nkT}}$ (Ω^{-1})	$\frac{1}{R_{sh}}$ (Ω^{-1})	$\frac{qI_0}{nkT}\,e^{\frac{qV_{oc}}{nkT}}$ (Ω^{-1})	$\frac{1}{R_{sh}}$ (Ω^{-1})	$I_0\,e^{\frac{qI_{sc}R_s}{nkT}}$ (A)	$\left(I_{sc} - \frac{V_{oc}}{R_{sh}}\right)$ (A)
A_1	0.139	998	$(2.71 \times 10^{-6}$–$5.32 \times 10^{-6})$	0.001	(2.56–6.21)	0.001	$(1.06 \times 10^{-7}$–$2.08 \times 10^{-7})$	(0.097–0.288)
A_2	0.124	998	$(2.61 \times 10^{-6}$–$4.77 \times 10^{-6})$	0.001	(2.56–6.21)	0.001	$(1.03 \times 10^{-7}$–$1.87 \times 10^{-7})$	(0.097–0.288)
B_1	0.153	998	$(3.24 \times 10^{-7}$–$7.67 \times 10^{-7})$	0.001	(2.67–7.47)	0.001	$(1.1 \times 10^{-8}$–2.6×10^{-8}	(0.097–0.288)

Table 5. Measured diode parameters of cell 1 using other methods and sets of four diode parameters formed with their different combinations.

	Method				Sets of diode parameters			
Diode parameters	[1]	[9]	[10]	[13]	C [1, 9]	D [9, 10]	E [9, 13]	F [9, 10, 13]
R_{sh} (Ω)	–	998	12.91	–	998	12.91	998	12.91
R_s (Ω)	0.265	–	0.354	0.130	0.265	0.354	0.130	0.130
n	–	1.31	–	1.405	1.31	1.31	1.405	1.405
I_0(A) $\times 10^{-8}$	–	0.709	–	–	0.709	0.709	0.709	0.709

the case. Similarly, the values of R_s could not be determined using Priyanka *et al*'s method [9] since we have restricted the *I–V* measurement on cell 1 to the 4th quadrant and have not measured the *I–V* characteristics in the 3rd quadrant. However, we have applied the methods of [1, 9, 10, 13] to the *I–V* data of cell 1 in 40–125 mW cm^{-2} intensity range to determine the diode parameters. These include the Araujo and Sanchez method [1] for R_s, Cueto method [13] for R_s and n, El-Adawi and Al-Nuaim method [10] for R_{sh} and R_s and Priyanka *et al*'s method [9] for R_{sh}, I_o and n. Following the authors [1, 10] we have also assumed $R_{sh} = \infty$ and $n = 1$ while applying the Araujo and Sanchez method [1] and $R_{sh} = \infty$ while applying the Cueto method [13]. On the other hand, we have assigned the values to n and I_0 as 1.52 and 7.56×10^{-8} A, respectively (from table 2, set A of our method) when applying the El-Adawi and Al-Nuaim method [10]. The values of diode parameters determined by these methods [1, 9, 10, 13] have been listed in table 5.

A comparison of tables 5 and 2 (set A1) shows that the values of diode parameters obtained by the above methods [1, 9, 10, 13] are significantly different than the values ($R_{sh} = 998$ Ω, $R_s = 0.139$ Ω, $n = 1.52$ and $I_0 = 7.56 \times 10^{-8}$ A) obtained by our method. The only exception is the value of R_{sh} determined by Priyanka *et al*'s method [9] which is same as obtained by our method. This is because the method of Priyanka *et al* [9] and our method are equivalent and use the same expression (as given by equation (15)) for determination of R_{sh} from the slope of illuminated *I–V* curve at the origin. On the other hand, the expressions used for determination of R_s, I_o and n in Priyanka *et al*'s method [9] and all the diode parameters (R_{sh}, R_s, I_o and n) in the other methods [1, 10, 13] are quite different than those used in our method.

The values of R_{sh}, R_s, I_o and n obtained by the above different methods and listed in table 5 were grouped to form four different sets of diode parameters. These sets (C, D, E, F) were then used in equation (1) to compute V_{oc} and CF values corresponding to the $I_{sc} = 228.6$ mA values of an experimental *I–V* curve of cell 1. The theoretical V_{oc} and CF values obtained using sets C, D, E and F are listed in table 6 along with the experimental values and the values obtained with our method (approach A, set A_1). It can be noted that all the sets C, D, E, F give values of V_{oc} and CF which are too deviated from the experimental values, whereas our method gives the values that match excellently with the experimental V_{oc} and CF values.

Thus, clearly our method (approach A, set A_1) is more accurate in comparison with the other analytical methods [1, 9, 10, 13] and is superior to them because it determines all the four diode parameters independently and without depending on any other method.

Application of the method to other cells

We have applied our method to determine the values of diode parameters of solar cells of a PV module 2577 of

Table 6. Comparison of values V_{oc} and CF for experimental curve and the theoretical *I–V* curves of cell 1 at 25 °C obtained using sets of diode parameters given in table 5 under a simulated AM1.5 solar radiation of 100 mW cm^{-2} intensity.

Performance	Values for sets					
parameters	Experimental	A1	C	D	E	F
V_{oc} (mV)	584.4	583.2	581.9	575.3	623.8	616.1
CF	0.718	0.717	0.696	0.572	0.745	0.620

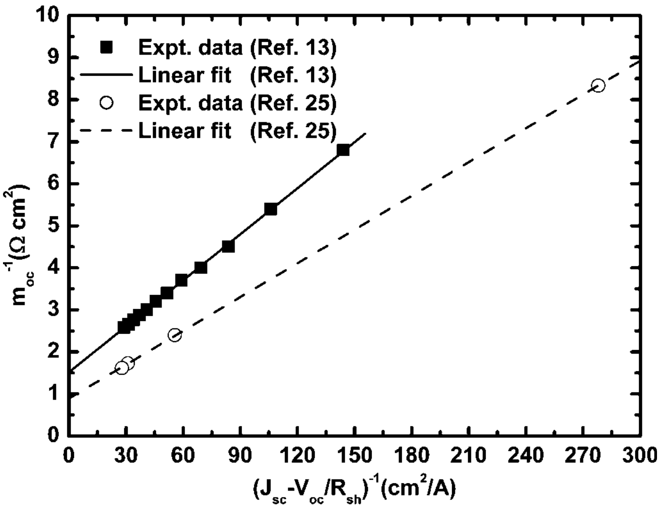

Figure 7. Plots of the m_{oc}^{-1} versus $(J_{sc}-V_{oc}/R_{sh})^{-1}$ curves using data of [13] (■) and [25] (○). The solid line gives a straight line fit to the data of 13 and the dashed line gives the straight line fit to the data of [25].

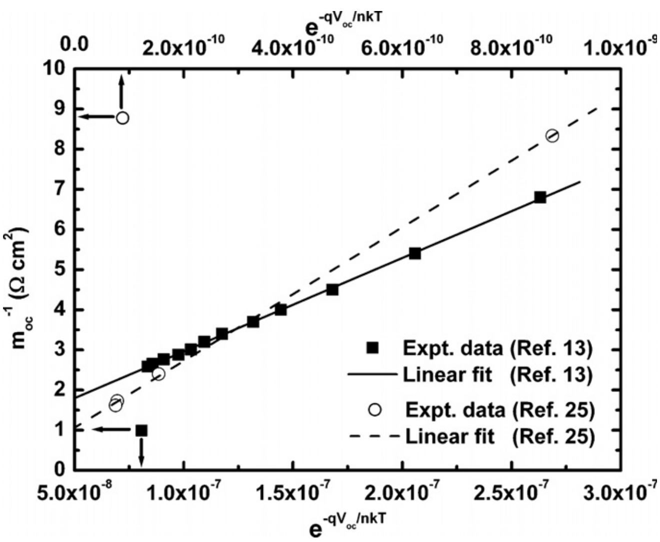

Figure 8. Plots of the m_{oc}^{-1} versus $e^{-qV_{oc}/nkT}$ curves using the data of [13] (■) and [25] (○). The solid line gives a straight line fit to the data of [13] and the dashed line gives the straight line fit to the data of [25].

Cueto [13] and a silicon solar cell of Mette *et al* [25]. The measurements of $(m_{oc})^{-1}$, J_{sc}, V_{oc} and CF by Cueto [13] on silicon PV modules and *J–V* characteristics by Mette *et al* [25] on silicon solar cells were done in 10–120 mW cm^{-2} intensity range. Here, we determine the slope of *J–V* curves at open

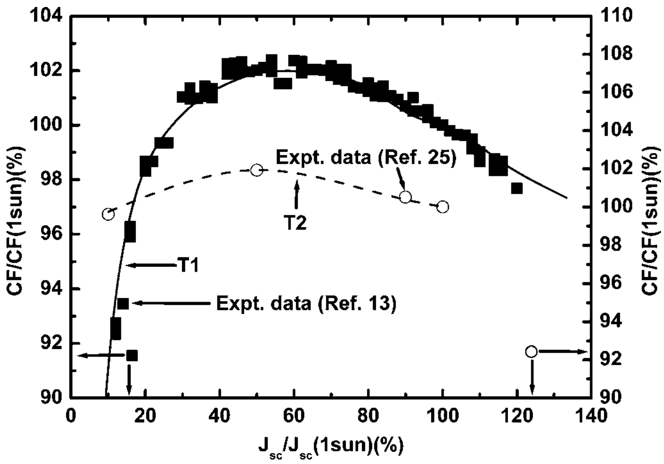

Figure 9. Comparison of theoretical and experimental variations of normalized CF of a PV module 2577 of [13] and that of a silicon solar cell of [25] with their respective normalized J_{sc} values. The values of CF and J_{sc} have been normalized with respect to their values at 1sun. The 1 sun value of J_{sc} was 30 mA cm^{-2} for an average cell of PV module 2577 of [13] and 36.3 mA cm^{-2} for cell of [25]. Symbol (■) denotes the experimental data of [13] and symbol (○) denotes the experimental data of [25]. Theoretical curves T1 (——) and T2 (– – –) have been generated by applying the present method to the data of [13] and [25] respectively.

circuit and short circuit conditions where J is current density (A cm^{-2}) Consequently, we obtain R_{sh}, R_s in the units of Ω cm^2 and reverse saturation current density J_0 (in the units of A cm^{-2}). The values of these diode parameters are listed in table 7. Following the observation of Cueto [13] the values of R_{sh} were taken to be 1000 Ω cm^2 for the cells of PV module 2577, whereas for cells of [25] R_{sh} was determined from the slope of *J–V* curve at short circuit conditions. Then values of R_s and n were determined from the m_{oc}^{-1} versus $(J_{sc}-V_{oc}/R_{sh})^{-1}$ curves as plotted in figure 7 and the values of J_o were determined from the slopes of the m_{oc}^{-1} versus $e^{-qV_{oc}/nkT}$ curves shown in figure 8. Thus, determined values of the diode parameters (R_{sh}, R_s, n, J_o) were used to generate *J–V* curves theoretically and thereby calculate the values of CF in the two cases. The theoretical and experimental values of CF values have been plotted in figure 9 against the J_{sc} values. Both the CF and J_{sc} values have been normalized with respect to their 1 sun values. The 1 sun values of J_{sc} were 30 mA cm^{-2} for an average cell of PV module 2577 of [13] and 36.3 mA cm^{-2} for cell of [25]. Theoretical curve T1 has been computed using the diode parameters determined by the present method using the data of an average cell of PV module 2577 of [13]. It can be noted that curve T1 matched very well the experimental CF data of PV module 2577 of [13] over the

Table 7. The values of diode parameters determined by our method using a silicon PV module no 2577 of [13] and a silicon solar cell of [25].

Silicon solar cell	R_{sh} (Ω cm^2)	R_s (Ω cm^2)	n	J_0 (A cm^{-2})
[13]	1000	1.514	1.415	2.441×10^{-9}
[25]	3300	0.894	1.043	3.215×10^{-12}

entire J_{sc} range of the study. Similarly, the theoretical curve T2 matched well with the experimental CF data of [25] over the entire range of J_{sc}. Thus, it is established that our method (approach A, set A_1) of measurement of diode parameters is applicable equally well to the isolated cells and the cells of a PV module.

Conclusion

We have evolved an analytical method of determining the representative values of all the diode parameters of a silicon solar cell using the values of slopes m_{sc} and m_{oc} of the *I–V* curves of cell at different intensities of the incident radiation in suitable intensity range. A combination of equations (15), (14) and (10) can be applied with high accuracy to determine values of R_{sh}, R_s, n and I_0 of a silicon solar cell analytically (with approach A, set A_1) in the P_{in} intensity range wherein I_{sc} increases linearly with P_{in} and both ε_1 and ε_2 have values much smaller than unity. Smaller the values of ε_1 and ε_2 better the accuracy of application of the method. For $\varepsilon_1 = \varepsilon_2 = 0.01$ the valid P_{in} range for cell 1 consisted of 1.91–204 mW cm^{-2}. Thus, the P_{in} range 40–125 mW cm^{-2} used for measurement of diode parameters of cell 1 in this work has been well within the valid P_{in} range. The theoretical *I–V* curves and CF values obtained using diode parameters determined with this method matched excellently with the experimental *I–V* curves and CF values of the cells obtained at different intensities in the 40–125 mW cm^{-2} range.

Acknowledgment

The authors are thankful to Professor Vikram Kumar, Director, National Physical Laboratory, New Delhi, for his permission to publish this paper. The author Firoz Khan gratefully acknowledges the support of CSIR.

References

[1] Araujo G L and Sanchez E 1982 *IEEE Trans. Electron Devices* **ED-29** 1511
[2] Ouennoughi Z and Chegaar M 1999 *Solid-State Electron.* **43** 1985
[3] Kaminski A, Marchand J J and Laugier A 1999 *Solid-State Electron.* **43** 741
[4] Radziemska E 2005 *Energy Convers. Manage.* **46** 1485
[5] Sinton R A, Kwark Y, Gan J Y and Swanson R M 1986 *IEEE Electron Device Lett.* **EDL-7** 567
[6] Green M A, Jianhua Z, Blakers A W, Taouk M and Narayanan S 1986 *IEEE Electron Device Lett.* **EDL-7** 583
[7] Cheknane A, Benyoucef B and Chaker A 2006 *Semicond. Sci. Technol.* **21** 144
[8] Rajkanan K and Shewchun J 1978 *Solid-State Electron.* **22** 193
[9] Priyanka, Lal M and Singh S N 2007 *Sol. Energy Mater. Sol. Cells* **91** 137
[10] El-Adawi M K and Al-Nuaim I A 2002 *Vac.* **64** 33
[11] Singh V N and Singh R P 1983 *J. Phys. D: Appl. Phys.* **16** 1823
[12] Agarwal S K, Muralidharan R, Agarwal A, Tewary V K and Jain S C 1981 *J. Phys. D: Appl. Phys.* **14** 1643
[13] Del Cueto J A 1999 *Sol. Energy Mater. Sol. Cells* **59** 393
[14] Cabestany J and Castaner L 1983 *J. Phys. D: Appl. Phys.* **16** 2547
[15] Chegaar M, Ouennoughi Z and Hoffmann A 2001 *Solid-State Electron.* **45** 293
[16] Bouzidi K, Chegaar M and Bouhemadou A 2007 *Sol. Energy Mater. Sol. Cells* **91** 1647
[17] Pysch D, Mette A and Glunz S W 2007 *Sol. Energy Mater. Sol. Cells* **91** 1698
[18] Datta S K, Mukhopadhyay K, Bandopadhyay S and Saha H 1992 *Solid-State Electron.* **35** 1667
[19] Kerr M J, Cuevas A and Campbell P 2003 *Prog. Photovolt., Res. Appl.* **11** 97
[20] Gaubas E and Vanhellemont J 2007 *J. Electrochem. Soc.* **154** H231
[21] Larin F 1968 *Radiation Effects in Semiconductor Devices* (New York, London, Sydney: Wiley) P 91
[22] Macdonald D and Cuevas A 2000 *Prog. Photovolt., Res. Appl.* **8** 363
[23] Jain G C, Prasad A and Singh S N 1974 *Solid-State Electron.* **17** 431
[24] Howard N R and Johnson G W 1965 *Solid-State Electron.* **8** 275
[25] Mette A, Pysch D, Emanuel G, Erath D, Preu R and Glunz S W 2007 *Prog. Photovolt., Res. Appl.* **15** 493